International Journal of Engineering Research and Science & Technology

ISSN 2319-5991 www.ijerst.com
© 2026 IJERST. All Rights Reserved
Peer Reviewed, Referred & Indexed Journal

Research Paper

SUNMOTION – INTELLIGENT SOLAR PANEL ROTATION

J. Prakash Patil
MTech LIMISTE, MIEEI
Assistant professor
Department of electronics and communication engineering
Vijay rural engineering college
Nizamabad, Telangana
sangeethaprakash2024@gmail.com

Nadkuda Akash
Student
Department of Electronics and Communication
Vijay rural engineering college
Nizamabad, Telangana
nadkudaakash1@gmail.com

Sidda Shashank
Student
Department of electronics and communication engineering
Vijay rural engineering college
Nizamabad, Telangana
siddashashank4@gmail.com

Nadipolla Srinath
Student
Department of electronics and communication engineering
Vijay rural engineering college
Nizamabad, Telangana
srinathnadipolla@gmail.com

Abstract*—SunMotion integrates four-quadrant illumination sensing, dual-axis photovoltaic panel positioning, embedded decision logic, and electrical-output monitoring in a unified solar-tracking configuration. Normalized differences of light-dependent resistor signals determine azimuth and elevation corrections, while angular limits and deadband control suppress unnecessary actuator movement. Synchronized voltage–current acquisition establishes the basis for power estimation, and auxiliary consumption is incorporated into the net-energy model. The developed system architecture includes a monitoring interface, operating-state supervision, and a fixed-orientation reference procedure. Evaluation combines mathematical analysis of incidence-angle effects, functional verification criteria, and quantitative findings from relevant solar-tracking investigations. The resulting engineering framework establishes traceable control and energy-assessment methods while distinguishing cited experimental findings from device-specific performance verification.

Keywords*—Photovoltaic systems; solar tracking; LDR sensors; dual-axis actuation; embedded control; net energy; monitoring; renewable energy.

I. INTRODUCTION

Photovoltaic (PV) systems convert incident solar irradiance into electrical energy, but the available direct-beam component is influenced by the angle between sunlight and the module normal. Fixed-tilt installations simplify mechanical construction; however, their orientation cannot follow both daily solar motion and seasonal changes. Solar tracking provides an alternative by adjusting the panel direction while accounting for mechanical motion, weather, and auxiliary power requirements [1]–[5].

A) Problem Formulation

SunMotion was structured to maintain favorable solar incidence through a compact, controlled rotation platform. Four design requirements guided the architecture: directional sensing, stable motor commands, safe angular travel, and traceable electrical measurements. Gross PV power alone does not characterize system performance because motors, control electronics, and optical sensing also consume energy. The analysis therefore uses net energy rather than isolated voltage measurements [6], [7].

B) Design Objectives and Scope

The developed architecture incorporates four LDR channels to determine relative illumination along the left–right and top–bottom directions. A microcontroller processes the sensor signals, selects correction directions, and drives azimuth and elevation actuators. Deadband logic and angular limits regulate movement, while voltage and current sensors form the electrical monitoring pathway. The monitoring dashboard organizes orientation, operating state, and energy-related measurements. Astronomical solar-position calculations provide an additional supervisory reference when integrated [8], [11].

The configuration represents an embedded electromechanical tracking system with distinct sensing, actuation, and monitoring functions. Actuator torque, controller thresholds, and electrical protection are specified in relation to the selected PV module and rotating structure. Structural loading, weather exposure, and protective circuitry are treated as engineering constraints independent of the optical tracking algorithm.

C) Research Contribution

The engineering contribution comprises a coordinated four-sensor comparison method, deadband-controlled dual-axis motion, and an energy-aware monitoring architecture. Its assessment procedure considers fixed-panel reference behavior, angular tracking error, auxiliary electrical consumption, and transient illumination. Experimental

energy improvements in the cited literature are compared separately from the analytical behavior of the SunMotion configuration [1], [3], [12].

D) System Boundaries

The SunMotion configuration is intended for a compact photovoltaic module on a movable support. Mechanical orientation control is distinct from maximum-power-point tracking (MPPT), which adjusts the electrical operating point of the PV module or associated converter. Mechanical tracking changes the optical incidence angle, whereas MPPT modifies voltage–current operation. Their contributions must be evaluated independently when both functions are incorporated [14], [15]. This distinction prevents changes in electrical load matching from being attributed to panel orientation.

The developed control structure also separates supervisory monitoring from motor safety. Telemetry and the operator interface assist diagnostics, while actuator travel limits remain effective independently of display or communication status. Data logging supports engineering verification rather than replacing local motion control.

II. RELATED WORK

A) Mechanical Configurations

Single-axis trackers typically rotate around one mechanical degree of freedom, whereas dual-axis mechanisms adjust both azimuth and elevation. Abdallah and Nijmeh [12] demonstrated programmable two-axis tracking, and Kalogirou [13] used LDR measurements in a motorized one-axis arrangement. Yao et al. [16] developed a dual-axis tracker with distinct tracking strategies. Reviews identify trade-offs among energy collection, structural cost, maintenance, angular accuracy, and motor duty cycles [1]–[5], [9], [10].

B) Sensing and Control Strategies

A tracker may estimate the solar position from time and coordinates, use optical sensors to detect illumination differences, or combine both approaches. Reda and Andreas [11] established an accurate astronomical solar-position algorithm. Sensor-based tracking has been studied using LDR circuits, servomotor actuation, and feedback mechanisms [13], [17], [24]. Comparative research also considers sensorless tracking through PV power measurements [14], [15]. Under clouds or partial shading, a light sensor can identify a locally bright direction that is not necessarily the direct solar position; filtering and supervisory logic are therefore important.

C) Net Energy and Intelligent Monitoring

Lazaroiu et al. [18] emphasized the auxiliary energy associated with low-power PV tracking. IoT-connected trackers extend the control function to data logging and visualization [20], [27]. Recent studies examine actuator wear, movement scheduling, and system reliability [22], [23]. Consequently, a scientifically meaningful comparison should log PV output and actuator consumption at equivalent times, irradiance conditions, and electrical loading. The control strategy should not assume that continuous motion is always preferable to interval-based adjustment.

D) Research Gap

The literature identifies limited reporting of sensor calibration, low-illumination operation, end-stop protection, and net electrical energy in elementary solar-tracking implementations. The SunMotion architecture addresses these technical aspects through a measurement–decision–actuation–verification sequence and explicit system verification criteria. Its subsystem organization follows established solar-tracker principles while permitting independent hardware assessment [3], [5], [21], [29].

E) Comparative Selection Criteria

Tracker configuration depends on module aperture, local solar resource, wind conditions, support stiffness, duty cycle, and maintenance requirements. Single-axis devices have fewer moving joints, while dual-axis arrangements offer an additional degree of freedom for solar elevation. Theoretical beam capture alone does not determine engineering performance because actuator consumption, bearing friction, sensor ageing, and calibration drift affect net yield [3], [4], [10]. The SunMotion two-axis configuration allows elevation motion to be disabled for a controlled single-axis comparison.

Photovoltaic output is also affected by irradiance spectrum, module temperature, partial shading, and the electrical operating point. Accordingly, using voltage alone as a proxy for generated energy can produce misleading conclusions. A matched fixed-panel reference, synchronized current measurement, and defined electrical load are essential for estimating a tracker-induced improvement rather than a weather-induced variation [18], [19].

III. MATERIALS AND METHODS

A) System Architecture

Fig. 1 summarizes the completed system-level architecture and signal paths. A photovoltaic module is supported on an azimuth–elevation mounting assembly. Four LDR channels form the optical sensing unit, and their analog outputs enter an Arduino-compatible microcontroller. The control stage supplies rotation commands to a motor interface connected to two actuators. A voltage–current sensing stage acquires PV electrical outputs, and a monitoring interface displays the resulting variables. Regulated power distribution separates logic and actuator requirements; a data logger organizes synchronized orientation and electrical observations.

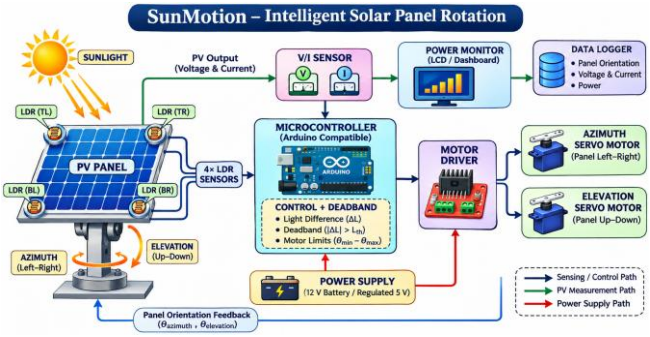


Fig. 1. SunMotion system architecture

B) Light-Sensor Processing and Rotation Control

Let L_TL, L_TR, L_BL, and L_BR denote the four calibrated sensor levels. The controller calculates normalized

left–right and top–bottom errors. Denominator regularization avoids a division instability at low irradiance. The following mathematical relations define the two control inputs:

$$e_az = \frac{(L_TR + L_BR) - (L_TL + L_BL)}{L_TR + L_BR + L_TL + L_BL + \varepsilon} \quad (1)$$

$$e_el = \frac{(L_TL + L_TR) - (L_BL + L_BR)}{L_TR + L_BR + L_TL + L_BL + \varepsilon} \quad (2)$$

For each axis, the controller issues motion commands only when the absolute normalized error exceeds the selected deadband. Error polarity determines the correction direction, while bounded actuator increments limit overshoot. A low-light condition invokes a stationary or stow state, and mechanical end stops constrain travel independently of software decisions. Rate-limited control updates suppress repeated reversals caused by sensor noise.

C) Electrical Power and Energy Accounting

At sample interval k, measured PV voltage and current determine instantaneous electrical power. Energy is evaluated through time-weighted sampling, which accounts for unequal observation intervals. A separate auxiliary-energy register represents consumption by the motors and control electronics:

$$P_avg = \frac{\Sigma\, P_k\, \Delta t_k}{\Sigma\, \Delta t_k} \quad (3)$$

The net-energy gain relative to a fixed panel must deduct the tracker auxiliary energy from the tracked PV energy. For a comparison period T, the gain is defined by:

$$G_net = \frac{E_trk - E_aux - E_fix}{E_fix} \quad (4)$$

The ratio in (4) is multiplied by 100 for percentage net-energy gain. Here E_trk denotes tracked photovoltaic energy, E_aux is auxiliary consumption, and E_fix is the fixed-reference photovoltaic energy. The comparative method uses equivalent module ratings, electrical loading, measurement calibration, and acquisition periods. Ambient irradiance, temperature, shading, and wind conditions are retained as explanatory variables [18], [20].

D) Hardware Integration and Safe Operation

TABLE I. SUNMOTION HARDWARE AND CONTROL FUNCTIONS

Module	Engineering function
PV module + two-axis support	Energy conversion and directional mounting
Four LDR channels	Illumination-gradient measurement
Microcontroller	Filtering, deadband, motion limits
Motor interface + actuators	Azimuth and elevation positioning
Voltage/current sensing	PV output acquisition
Display / data log	Telemetry and performance review
Regulated supply	Separated logic and actuator power

The hardware specification accounts for startup torque, gear and brake behavior, and aerodynamic loading. Cable strain relief is incorporated at moving joints. The electrical architecture identifies fusing, reverse-polarity protection, and separation of low-level PV measurements from motor switching disturbances. Watchdog and safe-state control address invalid sensor input and communication failures.

E) Control Sequence and Data Verification

The defined control sequence begins with sensor-channel verification and initialization of allowable angular travel. During daylight, the controller samples LDR channels, filters disturbances, computes both normalized errors, and updates motor actuation. Electrical power, panel orientation, and motor activity share a common acquisition time base. Low illumination activates a safe operating state. Reset and manual override functions remain bounded by angular limits, while calibration establishes sensor balance and actuator response.

F) Sensor Calibration and Signal Conditioning

The four optical channels require a common measurement scale. A practical calibration sequence records each LDR reading under approximately uniform illumination and estimates offsets or gain factors that equalize the response. The normalized error structure reduces common-mode dependence on overall brightness, but it does not compensate for severe sensor mismatch. A moving-average or median filter may reduce transient sensor noise; the filter length must remain short enough to preserve response to genuine solar movement.

In cloudy conditions, diffuse illumination can make the left–right and top–bottom differences small even though the panel is not ideally oriented. The controller therefore requires a minimum illumination threshold, a timeout for ambiguous gradients, and a safe hold strategy. A reference position based on a clock or a stored orientation can optionally limit cumulative drift, while a manual calibration routine allows correction after maintenance or mechanical disassembly. The position of the LDR head should be rigidly coupled to the panel normal so that its optical balance represents the panel orientation.

G) Actuator Torque and Mechanical Constraints

An azimuth–elevation mount should be sized according to the combined mass of the photovoltaic module and rotating structure, center-of-mass offset, frictional losses, and possible wind torque. A motor whose stall torque is only marginally above the static lifting torque may not provide reliable startup or safe braking. Gear reduction increases available torque but reduces angular speed; this trade-off is acceptable because solar motion is slow relative to normal electromechanical actuator response.

Angular-velocity and incremental-displacement constraints protect the mount, particularly near mechanical travel limits. Flexible cable routing limits torsional fatigue under repeated azimuth motion. Limit switches or independent position feedback provide additional safeguards beyond optical sensing. The mechanical specification also addresses corrosion, water ingress, and high-wind stow orientation. These features define hardware acceptance criteria for physical integration.

H) Power Budget and Energy Measurement

The electrical power balance includes microcontroller consumption, sensor and display consumption, motor electrical power during motion, and any converter losses. A position-holding actuator may draw nonzero current even when rotation is stopped; this component must not be omitted from energy accounting. Separate sensing of the PV output and auxiliary supply prevents motor transients from

being mistaken for photovoltaic fluctuations. A battery-powered research installation must additionally record state-of-charge changes to avoid attributing stored energy to solar conversion.

The acquisition strategy accounts for motor start-up current pulses while maintaining stable photovoltaic power estimation. A calibrated shunt or Hall-effect sensor provides current measurements; temperature drift, offset, and ADC quantization contribute to the uncertainty budget. Total energy is obtained by integration across the logging interval rather than extrapolating a single instantaneous power observation. Reference-meter calibration establishes measurement traceability.

I) Operating States and Fault Handling

The control implementation can be represented by five states: initialization, daylight tracking, stationary hold, low-light stow, and fault lockout. Transition to daylight tracking requires valid sensor and actuator conditions. The deadband produces a stationary hold state when both normalized errors are within tolerance. Low irradiance, excessive motor current, or an end-stop event forces a protective transition. The operator may request a manual state only when mechanical limits remain active.

Each operating-state transition is associated with a timestamp and event code, allowing solar-tracking movements to be distinguished from calibration or protective actions. Logger records use consistent physical units together with controller version and parameter settings. This organization prevents variations in deadband, sampling frequency, and gear ratio from obscuring comparisons between measurement periods.

J) Numerical Stability and Sampling Frequency

Because the sensor error is a ratio, the controller must guard against low denominator values. The regularizing constant ε is selected relative to the expected ADC scale, while measurements below a minimum combined irradiance threshold are treated as insufficient directional evidence. These safeguards avoid large commands arising from tiny differences between nearly dark sensors. Before installation, the controller should verify that every ADC channel remains within its electrical input limits and does not saturate under direct midday illumination.

Optical sensing and actuation use distinct update intervals. Multiple optical readings can be combined for an orientation decision, while electrical power is sampled more frequently during actuator operation. Bounded motor increments allow the mechanical assembly to settle before the next optical comparison. This reduces apparent oscillation caused by backlash, inertia, and temporary sensor shading.

IV. EXPERIMENTAL RESULTS

A) Comparative Research Evidence

Table II summarizes quantitative results obtained in earlier experimental solar-tracking investigations under different locations, seasons, and hardware conditions. These results provide an external technical comparison rather than a direct SunMotion prototype measurement, because the experimental protocols differ. Abdallah and Nijmeh [12] observed an improvement of up to 41.34% relative to a fixed reference. Fathabadi [15] reported seasonal energy gains of 27.7–42.7%, and Acosta-Banda et al. [29] reported an 18% improvement with an embedded tracking configuration.

TABLE II. SELECTED EXPERIMENTAL SOLAR-TRACKING FINDINGS

Reference	Tracking method	Reported result
[12]	PLC-driven two-axis	Up to 41.34% energy gain
[15]	Dual-axis sensor/sensorless	27.7–42.7% seasonal gain
[29]	Embedded control + vision	18% relative energy gain

B) Analytical Incidence-Angle Comparison

For direct-beam irradiance incident on a planar module, the geometric collection factor approximately follows the cosine of the incidence angle over the illuminated front hemisphere. Fig. 2 illustrates the theoretical relationship between solar incidence angle and normalized photovoltaic power. This relationship isolates geometric alignment and excludes diffuse irradiance, module temperature effects, electrical conversion losses, and ground-reflected radiation. It provides a physical explanation for the role of panel orientation in direct-beam energy collection.

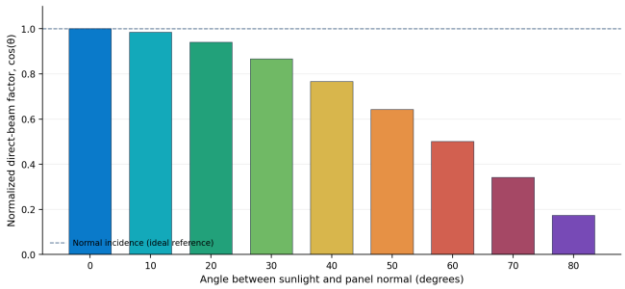


Fig. 2. Analytical normalized direct-beam factor versus panel incidence-angle error.

C) Evaluation Procedure and Metrics

The performance-evaluation protocol compares tracked and fixed-reference PV modules through synchronized samples collected over matched observation periods. Each record comprises time, irradiance, voltage, current, module temperature, azimuth, elevation, and actuator energy. The evaluation variables include mean angular error, average PV power, integrated gross energy, auxiliary electricity, net energy gain, and actuator movement count. Tests under clear and partially cloudy conditions distinguish tracking response from transient atmospheric variability [6], [18], [22].

TABLE III. SYSTEM VERIFICATION CRITERIA

Test case	Acceptance evidence
Uniform sensor illumination	No repeated motor oscillation
Left/right optical imbalance	Correct azimuth response
Top/bottom imbalance	Correct elevation response
Axis travel limit	Actuator safely stops
Low-light condition	Stow / hold state engages
Fixed vs tracked reference	Paired energy and auxiliary logs

D) Monitoring Interface Design

Fig. 3 illustrates the developed photovoltaic monitoring-interface layout and its measurement parameters. It organizes voltage, current, electrical power, angular

orientation, operating mode, and auxiliary energy into an operator-facing display. These variables are populated through the electrical sensing and data-acquisition pathway during instrumented operation. The embedded motor controller operates independently of the visualization layer, preserving local control during a dashboard or communication interruption.

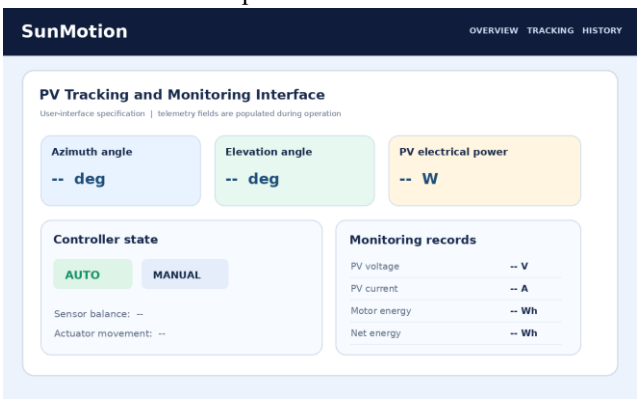


Fig. 3. SunMotion monitoring-interface layout for panel orientation and electrical data.

E) Interpretation and Limitations

The cited tracking experiments support the general benefit of improved solar orientation but do not determine a universal energy-gain value for SunMotion. Light-sensor mismatch, transient shading, mechanical backlash, and electrical interference influence the precision of directional control. Current-sensor offset, sampling synchronization, and variations in PV loading contribute to measurement uncertainty. The analysis therefore treats auxiliary-energy accounting and synchronized physical measurements as necessary conditions for valid performance comparison. Device-specific experimental validation remains necessary to quantify tracking performance and net energy yield.

F) Measurement Uncertainty and Experimental Controls

Energy-gain evaluation accounts for measurement accuracy and temporal variation. Voltage-sensor offset affects low-current power readings, while ADC noise and temperature drift influence other operating regions. Synchronized fixed and tracked measurements reduce cloud-related comparison errors. Sequential tests on a single module demand additional weather matching and cannot establish equivalent irradiance conditions solely through similar observation times.

Optical tracking error may be evaluated by comparing commanded panel orientation against a separately calculated solar position. The method should distinguish an angular deviation in azimuth from a three-dimensional incidence-angle error, since the two are not interchangeable. Weather and wind sensors can identify test intervals that should be excluded for safety or analyzed separately. Instrument specifications, calibration certificates, and uncertainty propagation belong in a complete experimental report.

G) Scenario-Based Functional Analysis

The system verification matrix in Table III establishes observable criteria for each operating state without assigning unverified numerical thresholds. Under adequate illumination, a controlled optical imbalance must generate the appropriate axis command and return toward sensor equilibrium. Within the deadband, repeated motor reversal is suppressed. At a travel limit, actuation stops despite any remaining optical error. Under low illumination, the operating sequence enters its specified stationary or stow condition.

Power-cycle verification examines whether the controller restarts without uncontrolled motor motion. A disconnected sensor must be identified as a fault rather than a bright directional measurement. Current-limited actuator-stall evaluation, conducted under appropriate electrical safeguards, establishes protective behavior. These checks distinguish operational reliability from geometric alignment performance.

H) Interpreting Comparative Energy Results

The literature values in Table II show that a substantial gross energy improvement is possible, but the percentage gain is sensitive to season, cloud cover, incidence-angle distribution, and the tracker reference geometry. A study reporting the highest increase at a particular location cannot be assumed to provide the highest gain for another site. Longer monitoring intervals are desirable because a tracker may improve morning and evening yield yet incur additional movement losses during periods when the irradiance is insufficient to offset actuation.

Electrical comparison should therefore report both energy harvested by the PV panel and energy delivered after subtracting controller and motor consumption. Environmental differences between the two modules must be minimized, and the power measurement interval should include standby consumption. Failure rates, maintenance frequency, weather-stow operation, and repeatability are further factors that determine whether an energy gain translates into a practical engineering benefit [4], [18], [22].

I) Reproducibility and Engineering Interpretation

Reproducibility is supported by recording PV nameplate ratings, sensor geometry, angular reference positions, motor-drive configuration, environmental conditions, and synchronized electrical measurements. Controller parameter records include the filtering interval, deadband, minimum illumination threshold, and motion limits. The analysis distinguishes gross PV production from auxiliary electrical expenditure. A matched single-axis comparison isolates the incremental effect of elevation tracking.

The monitoring interface provides structured inspection of the operating mode and measured electrical quantities; interface appearance alone is not evidence of tracking accuracy. Quantitative tracking performance is evaluated through synchronized physical measurements and appropriate reference conditions. The paper therefore separates the completed system architecture and analytical evaluation from the independently cited experimental performance comparisons.

J) Comparative Metrics and Reporting Units

The performance-reporting structure incorporates angular tracking metrics and electrical outcomes. Mean angular error is expressed in degrees, PV power in watts, and electrical

energy in watt-hours. Actuator duty cycle, movement count, and time spent in low-light hold provide additional operational measures. Each numerical value is associated with its unit, acquisition interval, and averaging method to maintain comparability across observation periods.

TABLE IV. ELECTRICAL AND CONTROL EVALUATION VARIABLES

Metric	Unit / assessment
Tracking error	Degrees; reference vs actual orientation
PV output power	W; synchronized voltage × current
Gross / auxiliary energy	Wh; integrated over matched periods
Net energy gain	%; after auxiliary consumption
Motor activity	Switching count, motion duration
Control reliability	End-stop, low-light, sensor-fault tests

A single peak-power measurement does not characterize daily tracking performance because PV output changes with irradiance and time. Integrated net energy across matched sampling intervals is the principal comparison variable. Supporting time-series figures include PV power, controller current, panel orientation, and incidence angle. Original timestamps permit orientation corrections to be distinguished from weather-related power fluctuations.

K) Environmental and Mechanical Sensitivity

Solar tracking imposes outdoor engineering requirements. Under high winds, a panel may require a predefined stow orientation that reduces aerodynamic loading; under heavy rainfall, the electrical enclosure must maintain protection against water ingress. Thermal expansion of joints and mounting brackets can change optical calibration over time. The LDR mount also needs a consistent shadow geometry because a change in barrier height or spacing modifies directional response even with unchanged firmware.

V. CONCLUSION

SunMotion was developed as an integrated system-level architecture combining four-quadrant light sensing, dual-axis motor control, photovoltaic measurement, and operator monitoring. Normalized illumination-difference feedback determines directional corrections, while deadband thresholds, angular limits, and low-light operating states establish a robust control sequence. The performance framework prioritizes net energy over instantaneous voltage or gross power alone. Experimental investigations in the cited literature demonstrate the potential for improved photovoltaic yield under favorable conditions, although gains depend on site conditions, tracking mechanisms, and auxiliary consumption. Device-specific energy yield and positioning accuracy require matched physical measurements before quantitative claims can be established. Further engineering extensions include astronomical reference tracking, position-encoder feedback, wind-stow supervision, and calibrated energy logging.

REFERENCES

[1] N. Kuttybay et al., "Assessment of solar tracking systems: A comprehensive review," Sustain. Energy Technol. Assess., 68, 103879, 2024. https://doi.org/10.1016/j.seta.2024.103879

[2] K. Kumba, P. Upender, P. Buduma, M. Sarkar, S. P. Simon, and V. Gundu, "Solar tracking systems: Advancements, challenges, and future directions: A review," Energy Rep., 12, 3566–3583, 2024. https://doi.org/10.1016/j.egyr.2024.09.038

[3] R. Sadeghi, M. Parenti, S. Memme, M. Fossa, and S. Morchio, "A review and comparative analysis of solar tracking systems," Energies, 18(10), 2553, 2025. https://doi.org/10.3390/en18102553

[4] A.-A. Petcut-Lasc, F.-M. Petcut, and V. E. Balas, "A systematic review of solar tracking systems for photovoltaic installations: Electrical performance, control strategies, and system integration," Electricity, 7(2), 45, 2026. https://doi.org/10.3390/electricity7020045

[5] H. A. Kazem, M. T. Chaichan, A. H. A. Al-Waeli, and K. Sopian, "Recent advancements in solar photovoltaic tracking systems: An in-depth review of technologies, performance metrics, and future trends," Solar Energy, 282, 112946, 2024. https://doi.org/10.1016/j.solener.2024.112946

[6] R. F. Fuentes-Morales et al., "Control algorithms applied to active solar tracking systems: A review," Solar Energy, 212, 203–219, 2020. https://doi.org/10.1016/j.solener.2020.10.071

[7] H. Mousazadeh, A. Keyhani, A. Javadi, H. Mobli, K. Abrinia, and A. Sharifi, "A review of principle and sun-tracking methods for maximizing solar systems output," Renew. Sustain. Energy Rev., 13(8), 1800–1818, 2009. https://doi.org/10.1016/j.rser.2009.01.022

[8] C.-Y. Lee, P.-C. Chou, C.-M. Chiang, and C.-F. Lin, "Sun tracking systems: A review," Sensors, 9(5), 3875–3890, 2009. https://doi.org/10.3390/s90503875

[9] A. Z. Hafez, A. M. Yousef, and N. M. Harag, "Solar tracking systems: Technologies and trackers drive types – A review," Renew. Sustain. Energy Rev., 91, 754–782, 2018. https://doi.org/10.1016/j.rser.2018.03.094

[10] W. Nsengiyumva, S. G. Chen, L. Hu, and X. Chen, "Recent advancements and challenges in solar tracking systems (STS): A review," Renew. Sustain. Energy Rev., 81, 250–279, 2018. https://doi.org/10.1016/j.rser.2017.06.085

[11] I. Reda and A. Andreas, "Solar position algorithm for solar radiation applications," Solar Energy, 76(5), 577–589, 2004. https://doi.org/10.1016/j.solener.2003.12.003

[12] S. Abdallah and S. Nijmeh, "Two axes sun tracking system with PLC control," Energy Convers. Manag., 45(11–12), 1931–1939, 2004. https://doi.org/10.1016/j.enconman.2003.10.007

[13] S. A. Kalogirou, "Design and construction of a one-axis sun-tracking system," Solar Energy, 57(6), 465–469, 1996. https://doi.org/10.1016/S0038-092X(96)00135-1

[14] H. Fathabadi, "Novel high accurate sensorless dual-axis solar tracking system controlled by maximum power point tracking unit of photovoltaic systems," Appl. Energy, 173, 448–459, 2016. https://doi.org/10.1016/j.apenergy.2016.03.109

[15] H. Fathabadi, "Comparative study between two novel sensorless and sensor based dual-axis solar trackers," Solar Energy, 138, 67–76, 2016. https://doi.org/10.1016/j.solener.2016.09.009

[16] Y. Yao, Y. Hu, S. Gao, G. Yang, and J. Du, "A multipurpose dual-axis solar tracker with two tracking strategies," Renew. Energy, 72, 88–98, 2014. https://doi.org/10.1016/j.renene.2014.07.002

[17] M. Saeedi and R. Effatnejad, "A new design of dual-axis solar tracking system with LDR sensors by using the Wheatstone bridge circuit," IEEE Sensors J., 21(13), 14915–14922, 2021. https://doi.org/10.1109/JSEN.2021.3072876

[18] G. C. Lazaroiu, M. Longo, M. Roscia, and M. Pagano, "Comparative analysis of fixed and sun tracking low power PV systems considering energy consumption," Energy Convers. Manag., 92, 143–148, 2015. https://doi.org/10.1016/j.enconman.2014.12.046

[19] S. Heslop and I. MacGill, "Comparative analysis of the variability of fixed and tracking photovoltaic systems," Solar Energy, 107, 351–364, 2014. https://doi.org/10.1016/j.solener.2014.05.015

[20] P. Muthukumar, S. Manikandan, R. Muniraj, T. Jarin, and A. Sebi, "Energy efficient dual axis solar tracking system using IoT," Meas.: Sensors, 28, 100825, 2023. https://doi.org/10.1016/j.measen.2023.100825

[21] P. Pawar, P. Pawale, T. Nagthane, M. Thakre, and N. Jangale, "Performance enhancement of dual axis solar tracker system for solar panels using Proteus ISIS 7.6 software package," Global Transitions Proc., 2(2), 455–460, 2021. https://doi.org/10.1016/j.gltp.2021.08.049

[22] U. Mamodiya and N. Tiwari, "Design and implementation of hardware-implemented dual-axis solar tracking system for enhanced energy efficiency," Eng. Proc., 59(1), 122, 2023. https://doi.org/10.3390/engproc2023059122

[23] D. A. Flores-Hernández, L. R. Islas-Estrada, and S. I. Palomino-Resendiz, "A novel tracking strategy based on real-time monitoring to increase the lifetime of dual-axis solar tracking systems," Appl. Sci., 14(18), 8281, 2024. https://doi.org/10.3390/app14188281

[24] Y. Boukdir and H. El Omari, "Novel high precision low-cost dual axis sun tracker based on three light sensors," Heliyon, 8(12), e12412, 2022. https://doi.org/10.1016/j.heliyon.2022.e12412

[25] A. Öztürk, S. Alkan, U. Hasırcı, and S. Tosun, "Experimental performance comparison of a 2-axis sun tracking system with fixed system under the climatic conditions of Düzce, Turkey," Turk. J. Electr. Eng. Comput. Sci., 24(5), 4383–4390, 2016. https://doi.org/10.3906/elk-1404-344

[26] S. Kumar, B. Singh, S. Banerjee, A. Raj, Devansh, and A. Gupta, "Performance comparison between Arduino based dual axis solar tracker and fixed module," J. Inf. Optim. Sci., 43(3), 475–480, 2022. https://doi.org/10.1080/02522667.2022.2044000

[27] M. K. A. Shamsuddin, N. S. Mohd Shah, F. A. Saparudin, A. A. A. Mohd Redzuan, and M. M. A. Noor Azeb, "Solar power system: Dual-axis tracker and monitoring system for a gateway station using Arduino and NodeMCU," Prog. Eng. Appl. Technol., 2(1), 612–622, 2021. https://periodical.uthm.edu.my/index.php/peat/article/view/873

[28] L. M. B. Rodrigues da Silva, M. P. Jeronimo dos Santos, T. S. de Sousa, and R. A. Beltrán, "Protótipo de rastreador solar de eixo duplo," Congr. Bras. Autom., CBA2022, 2022. https://doi.org/10.20906/CBA2022/3181

[29] A. Acosta-Banda et al., "Design, modeling, and experimental validation of a dual-axis solar tracking system with embedded control and monocular vision," Energies, 18(22), 5951, 2025. https://doi.org/10.3390/en18225951

[30] Shravya, G. Srikanth, T. Bhargavi, and A. T. P. S. Chandar, "Arduino-based dual-axis solar tracking and panel positioning system using light dependent resistor sensors," Eng. Heritage Sustain., 4(1), 69–76, 2026. https://doi.org/10.11591/ehs.v4i1.pp69-76